Local removal of oxygen for NAD(P)+ detection in aerated solutions

Thi Xuan Huong Le, Mathieu Etienne, François Lapicque, Alain Hehn, Neus Vilà, Alain Walcarius

Local removal of oxygen for NAD^+ detection in aerated solution

Thi Xuan Huong Le,[a] Mathieu Etienne,[a,]*François Lapicque,[b] Alain Hehn,[c] Neus Vilà,[a] Alain Walcarius[a]

[a] *Laboratoire de Chimie Physique et Microbiologie pour les Matériaux et l'Environnement (LCPME), UMR7564 CNRS – Université de Lorraine, 405 rue de Vandoeuvre, F-54600 Villers-lès-Nancy, France*

[b] *Laboratoire Réactions et Génie des Procédés (LRGP), UMR7274 CNRS – Université de Lorraine, 1 Rue Grandville, 54000 Nancy, France.*

[c] *Laboratoire Agronomie et Environnement (LAE), INRA - Université de Lorraine, 2 avenue de la forêt de Haye BP 20163, 54505 Vandoeuvre Cedex*

Abstract

The mediated electrochemical reduction of $NAD(P)^+$ in aerated solution was investigated and exploited for NAD(P)H regeneration in view of biosensing application. Oxygen was locally removed from the electrode surface with an electrochemical oxygen filter made of platinum grids positioned close to the oxygen sensitive reactions. The working electrode was a bucky paper functionalized with $[Cp^*Rh(bpy)Cl]^+$ by diazonium electrografting. The local oxygen removal was first evaluated, before to be applied to deoxygenation for NAD^+ and $NADP^+$ reduction. A porous silica gel layer encapsulating D-sorbitol dehydrogenase was finally deposited on the top of the modified bucky paper and the resulting bioelectrode was found sensitive to the presence of D-fructose.

Keywords: NAD(P)H; $[Cp^*Rh(bpy)Cl]^+$; diazonium electrografting; electrochemical oxygen filter; biosensor.

Correspondence (*): Dr. Mathieu Etienne mathieu.etienne@univ-lorraine.fr

1. Introduction

β-nicotinamide adenine dinucleotide NAD^+/NADH, and its phosphate derivative ($NADP^+$/NADPH) have been widely studied for their application in electrochemical biosensor and bioelectrocatalysis [1–5]. Indeed, there exists a large variety of NAD-dependent redox enzymes that can catalyze the electrochemical oxidation or electrochemical reduction of a large range of substrate [6].

For enzymatic catalysis, these enzymes provide a regio- and a stereoselectivity particularly that is powerful to synthetize complex molecules, with examples reported for dehydrogenase [7], P450 cytochromes with their reductase [8], etc. Electrochemistry should be of interest for the regeneration of the reduced form of the cofactor. The direct electrochemical reduction of $NAD(P)^+$ to NAD(P)H is however kinetically limited, and the low potential that must be used for allowing electron transfer reactions with the nicotinamide moieties induces side reactions and dimerization and thus inactivation of the enzymatic cofactor [9,10]. For that reason, redox catalysts have been evaluated and the complex $[Cp^*Rh(bpy)Cl]^+$ has been identified some decades ago to be particularly efficient for the electrocatalytic reduction of $NAD(P)^+$ to NAD(P)H [11].

Electrodes modified with this Rhodium complex have been developed, targeting specifically the electrochemical reduction of the nicotinamide cofactor, with modified conductive polymer matrices [12–14], and carbon nanomaterials [15,16]. More recently, we reported strategies of immobilization based on an initial step of diazonium electrografting [17–19]. A first strategy involved the electrografting of an azide containing molecule before conducting azide-alkyne Huisgen cycloaddition (click chemistry) to introduce a bipyridine group and a final complexation with the rhodium(III) metal [17]. We later introduced a simpler strategy by electrografting directly the bipyridine group on the surface of a bucky paper followed by a last step of complexation with rhodium [19].

The modified electrodes have been applied to NADH regeneration and D-sorbitol biosynthesis in an oxygen depleted solution, the removal of O_2 being achieved by purging the solution with N_2 and maintaining a nitrogen flow during the whole experiment [17, 19]. The reason is that oxygen can interfere with the reduction of NAD^+, which limits the accuracy of the electrochemical measurement [2], and can have deleterious effect on the catalyst or cofactor itself [20], which is highly problematic for biocatalytic applications.

Another major field of interest involving nicotinamide cofactors is related to biosensors [2]. In that case, the main target was the electrochemical oxidation of NADH or NADPH. Again, the electrochemical reaction is slow and a large variety of redox mediators have been proposed, immobilized on electrode and evaluated in electrochemical biosensors [21]. The reason to favor oxidation reactions is due to the absence of interference from molecular oxygen at the potential used for the biodetection. The interest of $NAD(P)^+$ reduction in biosensor application can only be evaluated in fully deoxygenated media.

Generally, methods for oxygen elimination can be sub-divided into four categories, (i) namely physical (purging the solution with nitrogen/argon flow in the solution), (ii) chemical (by adding oxygen reducing agent such as ascorbic acid [22] or sodium thiosulfate [23]), (iii) enzymatic (using glucose as oxygen scavenger in the presence of an enzyme to reduce oxygen molecules [24]), and (iv) electrochemical [25,26]. The latter can have some significant advantages, if small volumes have to be treated without introducing additional reactive species in the analyzed solution, *i.e.* without introduction of oxygen scavenger.

In this work, we have investigated the possibility of coupling local oxygen removal with $NAD(P)^+$ reduction for application in biosensing. The working electrode was a bucky paper functionalized with $[Cp^*Rh(bpy)Cl]^+$. It was obtained by diazonium electrografting of aminobipyridine followed by complexation of RhCp*Cl. It was covered by an electrochemical filter that allowed for local elimination of oxygen, according to an idea that we reported very

recently [27]. The effectiveness of oxygen removal was first checked in a background electrolyte solution and then in the presence of $NAD(P)^+$ to evaluate its interest for reductive cofactor regeneration in aerated solutions. The electrode was finally modified by D-sorbitol dehydrogenase and was found sensitive to D-fructose thanks to the electrochemical monitoring of NAD^+ that was produced when D-fructose was converted to D-sorbitol.

2. Experimental

2.1. Chemicals

Platinum grid (Pt, 0.12 mm nominal aperture, 0.04 mm wire diameter) and polyamide – Nylon grid (39 µm wire diameter, 50 µm nominal aperture) were purchased from Goodfellow, England. Multi-walled carbon nanotubes (MWCNT, > 95%, Φ 6-9nm, L 5µm), D-fructose (99 wt %), 3-glycidoxypropyltrimethoxysilane (GPS, 98%), β-nicotinamide adenine dinucleotide hydrate (NAD^+, ≥ 96.5%), β-nicotinamide adenine dinucleotide, reduced disodium salt hydrate (NADH, ≥ 97 %), pentamethylcyclopentadienylrhodium (III) chloride dimer ($(RhCp^*Cl_2)_2$), 1M hydrochloric acid solution, potassium chloride (99.99 %) were obtained from Sigma-Aldrich. Tetraethoxysilane (TEOS, 98%, Alfa Aesar), poly(ethylene imine) (PEI, 50% w/v in water, Mn = 60000, Fluka), sodium dihydrogen phosphate (99.5%, Merck), dichloromethane (Carlo Erba), glassy microfiber filters (0.26 mm thickness, 70 mm diameter, Whatman®) were used as received. Overproduction of N-His(6) D-sorbitol dehydrogenase (NHSD) (800 U mL^{-1}) was performed with Escherichia coli BL21GOLD (DE3) containing the corresponding expression-vectors pET-24a(+) (Novagen) and purification of the enzyme was performed with Histrap columns (GE Healthcare). All solutions were prepared with high purity water (18 MΩ cm) from a Purelab Option water purification system (Elga LabWater, Veolia Water STI, France).

2.2. Electrochemical device and procedure for oxygen removal from aqueous medium

The electrochemical cell was composed of four electrodes and fabricated from Teflon. Working electrode 1 (WE1) was a bucky paper or a glassy carbon electrode (GCE) and working electrode 2 (WE2) was made of one or a combination of two platinum grids (see Figure 1). These two working electrodes were separated by a nylon grid of less than 50 μm thickness. Glassy carbon was firstly wet-polished by SiC grinding paper (≠4000, Struers, Denmark) for 1 min, then cleaned with ethanol and distilled water under ultrasonic condition. The experiments were conducted with an Autolab PGSTAT 100 bipotentiostat in a four-electrode configuration (two working electrodes, Ag/AgCl/3M KCl reference electrode, and stainless steel counter electrode). The reaction of oxygen with the filter and the efficiency of the electrochemical removal was investigated by cyclic voltammetry. Usually, a 10 mL aqueous solution of KCl (0.1 M) was utilized as supporting electrolyte. When needed, purging the solution with N_2 gas was performed at least 15 min before running experiment and N_2 flow was kept over the solution during the experiment.

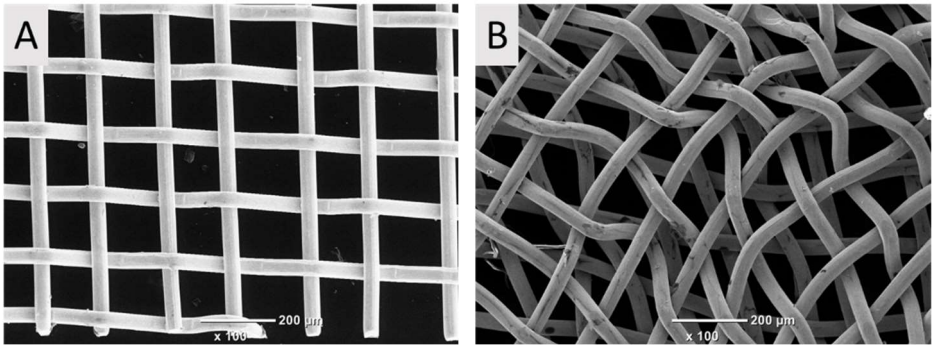

Figure 1. SEM pictures of platinum grids manufactured from (A) 1 or (B) 2 Pt layers.

2.3. Electrode modification, NAD(P)H regeneration procedure, and bioelectrode fabrication

The bucky paper electrode (BP) was prepared following the reported literature [28]. 10 mg MWCNT was dispersed in 50 mL ethanol by ultrasonication for 5 h. Afterwards, the suspension was decanted and vacuum filtered using the PVDF membrane filter. Then, the material was dried at 50 °C overnight. Finally, the electrode was cut at the suitable size before use. The immobilization of $[Cp^*Rh(bpy)Cl]^+$ (BP-Bpy-Rh) was prepared following the protocol published in a previous article [19]. This functionalized electrode was used for NAD^+ or $NADP^+$ reduction by observation of the catalytic peak on BP-Bpy-Rh during NAD^+/$NADP^+$ addition as schematically shown in Figure 2. Oxygen removal was achieved by applying a constant potential (-0.4 V vs. Ag/AgCl) at the oxygen filter (WE2). The catalytic response was evaluated by running cyclic voltammetry from -0.4 V to -0.9 V vs. Ag/AgCl at 5 mV s^{-1} scan rate.

For the detection of D-fructose, a compact cell was designed, including different layers. First, D-sorbitol dehydrogenase (DSDH) in silica gel, called here DSDH sol was deposited on a microfiber filter layer. The DSDH sol was synthesized by stirring overnight a mixture of 0.13 g GPS, 0.18 g TEOS with 0.5 mL water and 0.625 mL 0.01 M HCl [29]. The following day, the sol was diluted three times before mixing 40 µL of this medium with 20 µL PEI (20%) solution, 20 µL water and 30 µL of DSDH stock solution. The obtained DSDH gel layer was allowed to dry at 4 °C overnight, then was placed directly on the top of the oxygen filter. Before experiments, 1 mM NADH was mixed in 10 mL of buffer phosphate solution (PBS, 50 mM, pH 6.5). The biosensor response was evaluated by cyclic voltammetry, by introduced gradually D-fructose in the medium (in 50 mM PBS at pH 6.5).

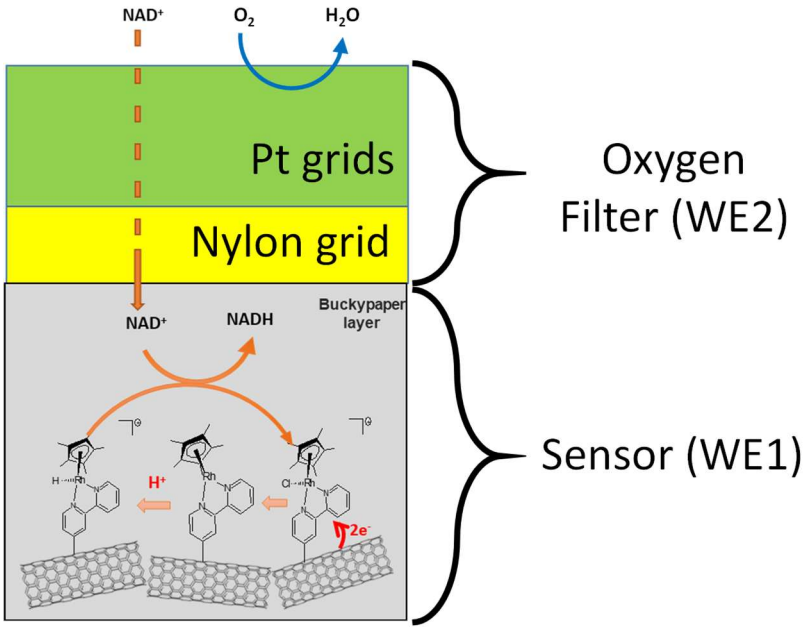

Figure 2. Principle of NAD^+ reduction on $[Cp^*Rh(bpy)Cl]^+$ functionalized bucky paper electrode acting as sensing element (working electrode 1, WE1) combined with an electrochemical O_2 filter (working electrode 2, WE2). The electrochemical filter is composed of platinum grids separated from the sensor using a Nylon grid.

3. Results and discussion

3.1. Local oxygen removal

The electrochemical reduction of oxygen at the platinum grids used to filter oxygen was investigated by cyclic voltammetry from 0 V to -0.9 V vs. Ag/AgCl at scan rate of 5 mV s^{-1} using 100 mM KCl as supporting electrolyte (Figure 3). In aerated solution (Fig. 3A), two regions can be distinguished in the CV: from -0.1 V to -0.4 V, the negative current plateau is attributed to oxygen reduction under diffusion control, whereas the cathodic current "wall" starting at -0.8 V is related to hydrogen evolution. Narrowing the potential window to the range from 0 to - 0.5 V allowed H_2 production to be avoided, with unchanged current plateau (Fig. 3A, blue curve). The filter was composed of either one or two platinum grids. The current recorded on the two-grid layer (red curve) was higher than that with a single Pt grid (black

curve). This increase can be explained by the larger electrode surface area available when more platinum is used, and also the larger volume that is treated by the porous electrodes [30], allowing a more efficient removal of oxygen. The experiment was repeated under N_2 medium for two Pt grids (Fig. 3B), showing the complete vanishing of the current profile from -0.1 V to -0.4 V. This clearly demonstrates that the plateau visible in Figure 3A (0 to - 0.5 V potential region) corresponds to oxygen reduction reaction. Moreover, the large current observed in the range of -0.7 V and -0.9 V attributed to hydrogen evolution was still visible. The potential at which the filter can be poised is thus comprised between the potential at which O_2 is reduced (lower than -0.2 V) and the potential of hydrogen evolution (higher than -0.7V). The potential of -0.4 V was chosen as the optimal one to apply to the platinum filter in order to evaluate its ability to remove oxygen from the surface of the sensor.

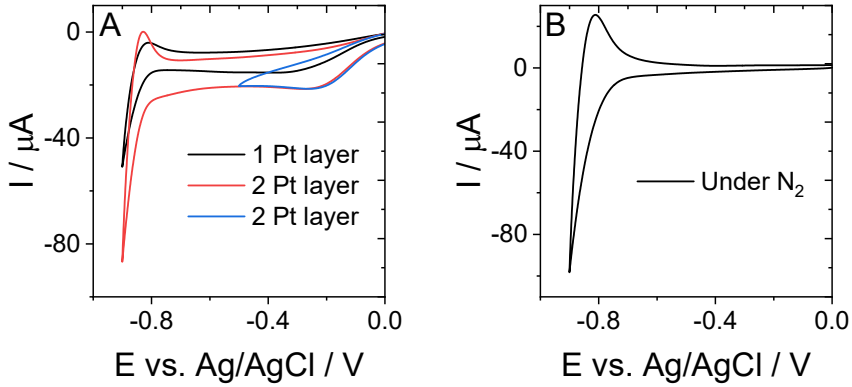

Figure 3. Cyclic voltammograms recorded in 100 mM KCl at a scan rate of 5 mV s^{-1}between 0 to -0.9V or 0 to -0.5V vs Ag/AgCl, using (A) Pt grids (one or two) in aerated solution (i.e., presence of O_2) and (B) two Pt grids under N_2 (i.e., absence of O_2).

First evaluation of the electrochemical scrubber for oxygen removal was carried out with a glassy carbon disk acting as sensor (WE1) and the platinum grids (one or two) as oxygen filter (WE2). In such experiment, the presence of oxygen was thus detected on WE1, whereas this

species is expected to be consumed on WE2. When the filter was not connected to the electrochemical cell (OFF position), large negative currents corresponding to oxygen reduction were observed at GCE surface in aerated solution, with values as high as -6 µA (-35 µA/cm^2) at -0.6 V (Fig. 4A). When the filter was ON, this current vanished. Figure 4B provides a closer look on the residual current in three different conditions: oxygen was effectively removed when applying a constant potential (-0.4 V) at the filter made with one Pt layer (black curve) or two Pt layers (red curve). In accordance to the higher reduction current (in absolute value) on the two Pt-layer electrode, O_2 removal was more efficient than with a single Pt grid, as revealed by the less significant residual currents, lower than 0.4 µA at 0.6 V. After degassing the solution under N_2 bubbling (blue curve), the current recorded on GCE (with oxygen filter WE2 on OFF position) was very similar to that obtained in aerated solution with the 2-grid layer (with oxygen filter WE2 in the ON position), which demonstrates the efficiency of the electrochemical scrubber for oxygen removal. According to a simple modeling of the electrochemical filter, the amount of residual oxygen can be rapidly lowered to less than 1 % of its initial concentration in less than few minutes [27]. This result is very promising in view to conducting experiments sensitive to the presence of oxygen, such as the electrochemical detection of NAD(P)$^+$.

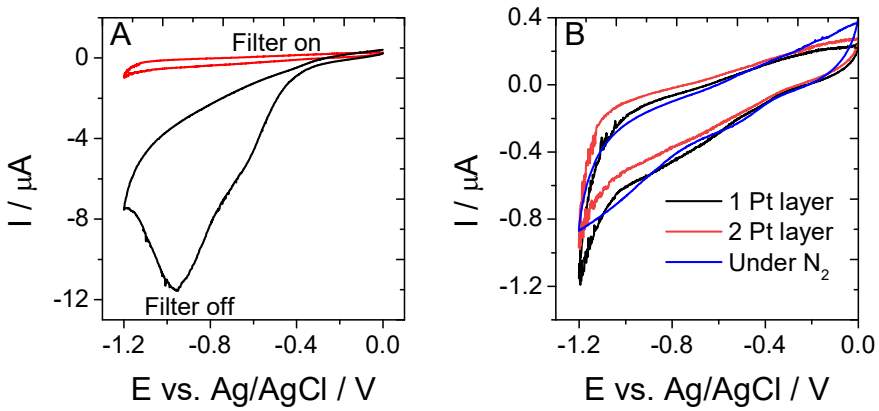

Figure 4. (A) Cyclic voltammograms recorded on GCE with (filter ON) and without (filter OFF) polarization of the oxygen filter (two platinum grids) at -0.4 V. (B) Cyclic

voltammograms recorded in 100 mM KCl (aerated solution, oxygen concentration in solution is in the range of 200-300 µM) at 5 mV s^{-1} in the potential region corresponding to oxygen reduction using GCE as WE1 (working electrode 1) while applying -0.4 V vs Ag/AgCl to the oxygen filter made of one or two platinum grids (acting as WE2); for comparison purpose, a CV curve was also recorded under N_2 (deaerated solution).

3.2. NAD(P)H regeneration and applications to enzymatic reactions

For $NAD(P)^+$ reduction, $[Cp^*Rh(bpy)Cl]^+$ (as immobilized onto bucky paper) was chosen as an efficient non-enzymatic catalyst because of its ability to lower overvoltage for the reduction of $NAD(P)^+$ to NAD(P)H [11]. By applying a suitable cathodic potential to the BP-Bpy-Rh electrode, Rh(III) centers on the surface of electrode can be reduced to Rh(I) before fast protonation from the buffer solution, and the resulting Rh-hydride species are likely to reduce $NAD(P)^+$ [31]. The catalytic response of $[Cp^*Rh(bpy)Cl]^+$ was investigated by cyclic voltammetry in 10 mL PBS solution at pH 6.5, respectively with the oxygen filter on ON and OFF positions, as illustrated in Figure 5. Oxygen concentration in solution is in the range of 200-300 µM, and depends on several parameters such as ionic strength, temperature and atmospheric pressure. Potential interference can be in principle observed for this range of concentration, and for that reason, the next experiments consider the effect of oxygen and the removal of oxygen on the detection of 250 µM NAD^+.

Control experiments were first performed without NAD^+ (Fig. 5A) using the Rh-based sensor and the electrochemical oxygen filter made with two platinum grids. Applying reduction potential (-0.4 V) to the platinum-based filter for oxygen removal (ON position) allowed the electrochemical response of Rh(III) complex to be observed at -0.65 V (black curve). A very similar voltammogram was recorded from a nitrogen-deaerated solution (red curve). Without $[Cp^*Rh(bpy)Cl]^+$ immobilized on the bucky paper, the above cathodic signal was not observed

(green curve). A clear interference from oxygen was evidenced when the oxygen filter was switched OFF, via a broad current peak observed in the range from -0.4 V to -0.7 V corresponding to the reduction of dissolved oxygen (blue curve in Fig. 5A) which is now likely to easily reach the sensor surface. The presence of oxygen masked thus the smaller signal from the rhodium catalyst immobilized on the sensing electrode.

In the presence of $NAD(P)^+$, the BP-Bpy-Rh electrode is known to provide an electrocatalytic response as the protonated Rh(I) species generated on WE1 can transfer a hydride ion to $NAD(P)^+$ for its reduction to NAD(P)H [32]. Thanks to this process, the cofactor can be regenerated and Rh(I) can be re-oxidized for long-term use. As shown in Figure 5B, the addition of 0.25 mM of NAD^+ to the PBS solution with the above WE2 at -0.4 V resulted in an increase of the cathodic current together with a small negative shift of the cathodic peak from -0.65 V to -0.75 V (Fig. 5B, black curve), consistent with the literature [33], confirming the successful reduction of NAD^+ to NADH. Once again, NAD^+ detection was repeated with degassed solution by N_2 bubbling, yielding very comparable voltammograms (Fig. 5B, red curve). NAD^+ reduction can be performed under air atmosphere by using the electrochemical oxygen filter made of two platinum grids. When the filter was switched OFF, a similar broad current peak observed in the range from -0.4 V to -0.7 V corresponding to reduction of dissolved oxygen was again observed and hindered the electrochemical detection of NAD^+ (Fig. 5B, blue curve). In addition, the interference of oxygen is not related only to this increased current that may lead to overestimation of the current due to $NAD(P)^+$ reduction. Indeed, Tosstorff et al. mentioned in their report that the reaction of the mediator with oxygen can lead to the formation of partially reduced oxygen, potentially harmful, and that the rhodium mediator [Cp*Rh(I)(bpy)H]+ was not stable in the presence of oxygen [20].

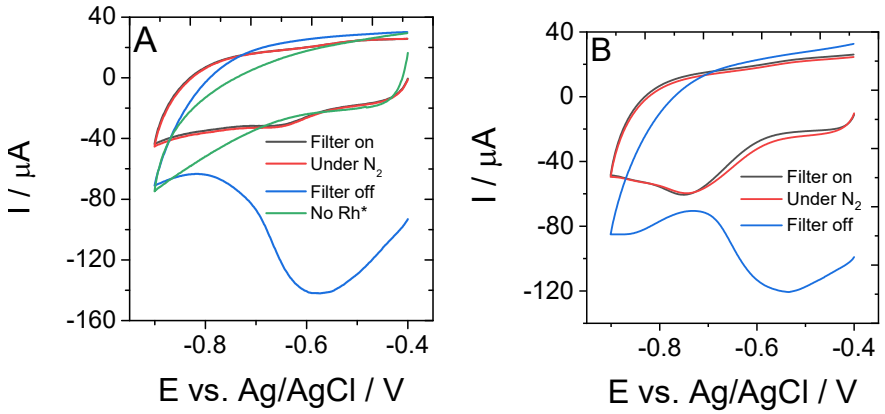

Figure 5. Cyclic voltammograms recorded at 5 mV s^{-1} using a $[Cp^*Rh(bpy)Cl]^+$ functionalized bucky paper (BP-Bpy-Rh) electrode (working electrode 1, WE1) in 50 mM PBS buffer at pH 6.5, and applying -0.4 V vs Ag/AgCl at the oxygen filter (working electrode 2, WE2): (A) without NAD^+ and (B) with 0.25 mM NAD^+ in the medium. Experiments have been performed either after a purge with nitrogen (Under N_2) or in the presence of O_2 with the filter active (Filter on) or inactive (Filter off). A control experiment performed with bucky paper without rhodium under N_2 is also reported (No Rh*).

Beside NAD^+ reduction, the oxygen filter WE2 was also used to examine the possible detection of the $NADP^+$ cofactor, as illustrated in Figure 6. To this end, amounts of $NADP^+$ at 0 mM, 0.5 mM, 1 mM, 1.5 mM, 2 mM, 3 mM and 4 mM, were gradually added into the buffer solution (50 mM PBS, pH = 6.5) and the two Pt grids of oxygen filter were set at -0.4 V vs Ag/AgCl. The cathodic peak rose from 10.5 µA without cofactor up to 77 µA in the presence of 4 mM $NADP^+$ (Fig. 6A). The negative shift in potential of the reduction peak with increasing $NADP^+$ concentration is indicative of an EC mechanism. The calibration curve shows a linear relationship between the peak current and the concentration from 0.5 to 3 mM (Fig. 6B). Beyong this value the slope decreases because of the limitation in the heterogeneous electron

transfer kinetics (as reported in previous work [17,19,31]), and the cathodic peak is progressively shifted to more negative potentials (from -0.65 V to nearly -0.85 V *vs*. Ag/AgCl) with increasing the $NADP^+$ concentration.

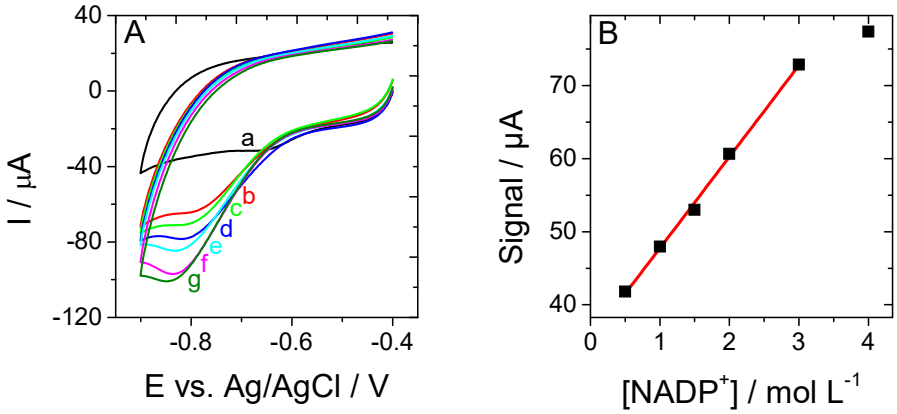

Figure 6. (A) Cyclic voltammograms recorded at 5 mV s^{-1} in 50 mM PBS buffer at pH 6.5 on the $[Cp^*Rh(bpy)Cl]^+$ functionalized bucky paper (BP-Bpy-Rh) electrode (working electrode 1, WE1) with $NADP^+$ gradually introduced at (a) 0 mM, (b) 0.5 mM, (c) 1 mM, (d) 1.5 mM, (e) 2 mM, (f) 3 mM and (g) 4 mM. (B) Corresponding calibration curve. The oxygen filter was composed of two platinum grids (working electrode 2, WE2); it was set at -0.4 V vs Ag/AgCl in all measurements. The signal reported here is the difference between the peak and the background current for each curve.

After successfully testing the reduction of NAD^+ and $NADP^+$ thanks to the electrochemical filter of oxygen, the functionalized BP-Bpy-Rh electrode was exploited for electrochemical detection of D-fructose. This analysis required the presence of D-sorbitol dehydrogenase (DSDH) [29]. To avoid any interaction between the rhodium catalyst and the surface functional groups of the enzyme (which could cause their degradation [19,34]), the catalyst and the enzyme have been separated by confining them in two different layers in the bioelectrode, as follows. DSDH encapsulated in a silica gel (see Section 2.3) was spread out onto a microfiber

filter layer: this layer was placed directly on the oxygen filter (WE2), thus at a short distance from the BP-Bpy-Rh sensor surface (WE1). The effectiveness of the bioelectrochemical reaction was checked by cyclic voltammetry on WE1 whereas the 2 Pt grids of WE2 were polarized at -0.4 V vs Ag/AgCl. The bioconversion was initiated by adding D-fructose to the PBS solution containing 1 mM of NADH. NAD^+ species generated by the enzymatic process left the gel layer, diffused through the porous structures of WE2 and the nylon separator to reach the surface of the sensor, where they were reduced into NADH. As shown in Figure 7, the cathodic current increased gradually upon increasing the D-fructose concentration up to 4 mM, to reach a saturation value near 25 µA. An apparent Km value was estimated to be 0.5 mM, i.e. in the range of previous estimation with similar immobilization protocols [19]. Moreover, even though oxygen was present in a large part of the cell solution and near the DSDH-containing layer, the oxygen filter located between the enzyme layer and the BP-Bpy-Rh sensing element allowed the effective local oxygen removal from the solution, which was beneficial for NAD^+ detection.

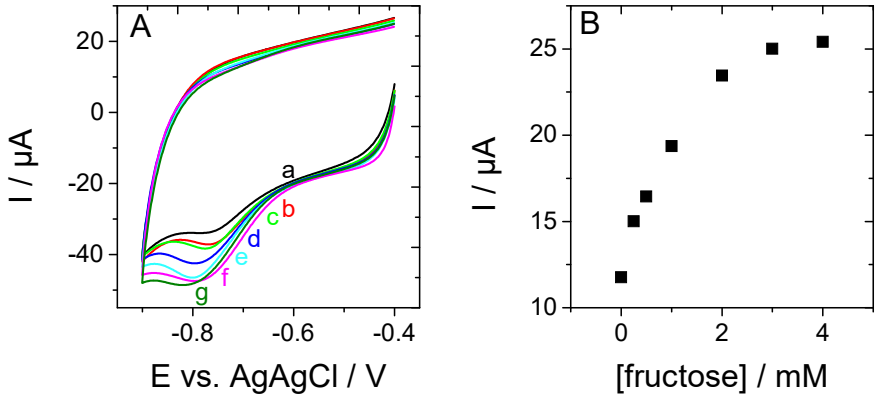

Figure 7. (A) Cyclic voltammograms recorded at 5 mV s^{-1} in 50 mM PBS buffer with 1 mM NADH at pH 6.5 using the $[Cp^*Rh(bpy)Cl]^+$ functionalized bucky paper (BP-Bpy-Rh) electrode (working electrode 1, WE1) coated with the oxygen filter composed of two platinum grids (working electrode 2, WE2, set at -0.4 V vs Ag/AgCl in all measurements), overcoated with the gel DSDH layer. D-fructose was gradually introduced in the cell solution from (a) 0

mM to (b) 0.25 mM, (c) 0.5 mM, (d) 1 mM, (e) 2 mM, (f) 3 mM and (g) 4 mM. (B) Corresponding calibration curve. The signal reported here is the difference between the peak and the background current for each curve.

During this study, we identified two potential drawbacks of this filter. The first one is the possible production of H_2O_2 [35] and reactive oxygen species [36]. Even if this cannot be excluded, we did not observe in this set of experiments evidences of interference from such species on NAD^+ detection. Platinum is probably one of the best materials for filter fabrication due to its catalytic properties for oxygen reduction reactions, limiting the production of harmful reactive species which could originate from an incomplete reduction of O_2. The second drawback is related to pH modification in the small volume of solution that is between the filter and the sensor surface. Measuring this local pH is not trivial and we have considered this question in a recent report based on simple calculations: it came out that a pH shift could be contained by using a small buffer concentration [27].

4. Conclusion

The electrochemical reduction and detection of $NAD(P)^+$ can be successfully performed in the absence of oxygen. Here, we have demonstrated the possibility of avoiding the removal of oxygen from the entire solution volume, by providing a way to remove it only from the surface of the electrode, in order to detect this enzymatic cofactor with a sensor made of a bucky paper electrografted with $[Cp^*Rh(bpy)Cl]^+$. This was achieved by using an electrochemical filter made of porous platinum grids, separated from the sensor surface by an insulating porous layer, a nylon grid. We have shown that oxygen was efficiently removed from the solution near the sensor surface. This allowed the detection of NAD^+ at a concentration as low as 0.25 mM, which was not possible in the presence of oxygen. The sensor was also likely to detect $NADP^+$

in the 0.5 to 4 mM concentration range. Finally, the detection of NAD^+ was combined with the enzymatic activity of D-sorbitol dehydrogenase encapsulated in a silica gel overlayer and this bioelectrode was found sensitive to increasing concentrations of D-fructose from 0.25 to 4 mM. Despite, the possible drawback associated with the system (risk of production of H_2O_2 and reactive oxygen species, local pH modulation, additional technical complexity that can bring more variability in the measurement), this strategy opens a new door for the development of novel bioelectrocatalytic devices implementing both an oxygen sensitive electrochemical reaction and an enzymatic system requiring the presence of molecular oxygen to operate, e.g. P450 cytochromes.

Acknowledgements

This work was supported partly by the French PIA project « Lorraine Université d'Excellence », reference ANR-15-IDEX-04-LUE. We gratefully acknowledge Gert W. Kohring from Saarland University (Saarbrucken, Germany) for providing D-sorbitol dehydrogenase.

References

[1] F. Hollmann, K. Hofstetter, A. Schmid, Non-enzymatic regeneration of nicotinamide and flavin cofactors for monooxygenase catalysis., Trends Biotechnol. 24 (2006) 163–171. doi:10.1016/j.tibtech.2006.02.003.

[2] L. Gorton, P.N. Bartlett, NAD(P)-Based Biosensors, in: P.N. Bartlett (Ed.), Bioelectrochemistry Fundam. Exp. Tech. Appl., John Wiley & Sons, Ltd, Chippenham, 2008: pp. 157–198.

[3] F. Hollmann, I.W.C.E. Arends, K. Buehler, Biocatalytic Redox Reactions for Organic Synthesis: Nonconventional Regeneration Methods, ChemCatChem. 2 (2010) 762–

782. doi:10.1002/cctc.201000069.

[4] X. Dominguez-Benetton, S. Srikanth, Y. Satyawali, K. Vanbroekhoven, D. Pant, Enzymatic Electrosynthesis: An Overview on the Progress in Enzyme- Electrodes for the Production of Electricity, Fuels and Chemicals, J. Microb. Biochem. Technol. S6 (2013) 007. doi:10.4172/1948-5948.S6-007.

[5] L. Zhang, M. Etienne, N. Vilà, A. Walcarius, Functional electrodes for enzymatic electrosynthesis, 2017. doi:10.1142/9781786343543_0006.

[6] P. Kornberger, F. Giffhorn, G.-W. Kohring, M.C. Flickinger, Dehydrogenases, Electrochemical Cofactor Regeneration, in: Encycl. Ind. Biotechnol., John Wiley & Sons, Inc., 2010: pp. 1888–1898. doi:10.1002/9780470054581.eib254.

[7] C. Kohlmann, W. Märkle, S. Lütz, Electroenzymatic synthesis, J. Mol. Catal. B Enzym. 51 (2008) 57–72. doi:10.1016/j.molcatb.2007.10.001.

[8] A. Hehn, U. De Picardie, J. Verne, U. Matern, Biosynthesis of coumarins in plants : a major pathway still to be unravelled for cytochrome P450 enzymes, (2016). doi:10.1007/s11101-006-9040-2.

[9] C.S. Morrison, W.B. Armiger, D.R. Dodds, J.S. Dordick, M.A.G. Koffas, Improved strategies for electrochemical 1,4-NAD(P)H2regeneration: A new era of bioreactors for industrial biocatalysis, Biotechnol. Adv. (2017). doi:10.1016/j.biotechadv.2017.10.003.

[10] F. Hildebrand, C. Kohlmann, A. Franz, S. Lütz, Synthesis, Characterization and Application of New Rhodium Complexes for Indirect Electrochemical Cofactor Regeneration, Adv. Synth. Catal. 350 (2008) 909–918. doi:10.1002/adsc.200700505.

[11] R. Ruppert, S. Herrmann, E. Steckhan, Efficient indirect electrochemical in-situ regeneration of nadh:electrochemically driven enzymatic reduction of pyruvate catalyzed by D-LDH, Tetrahedron Lett. 28 (1987) 6583–6586. doi:10.1016/S0040-4039(00)96919-3.

[12] S. Cosnier, H. Gunther, A polypyrrole [RhIIIC5Me5(bpy)Cl]+ modified electrode for the reduction of NAD+ cofactor, J. Electroanal. Chem. Interfacial Electrochem. 315 (1991) 307–312. doi:10.1016/0022-0728(91)80079-6.

[13] M. Beley, J.-P. Collin, Electrochemical regeneration of nicotinamide cofactor using a polypyrrole rhodium bis-terpyridine modified electrode, J. Mol. Catal. 79 (1993) 133–140. doi:10.1016/0304-5102(93)85096-C.

[14] J.H. van Esch, M.A.M. Hoffmann, R.J.M. Nolte, Reduction of Nicotinamides, Flavins, and Manganese Porphyrins by Formate, Catalyzed by Membrane-Bound Rhodium Complexes, J. Org. Chem. 60 (1995) 1599–1610. doi:10.1021/jo00111a018.

[15] B. Tan, D.P. Hickey, R.D. Milton, F. Giroud, S.D. Minteer, Regeneration of the NADH Cofactor by a Rhodium Complex Immobilized on Multi-Walled Carbon Nanotubes, J. Electrochem. Soc. 162 (2015) H102–H107. doi:10.1149/2.0111503jes.

[16] J.S. Lee, S.H. Lee, J. Kim, C.B. Park, Graphene–Rh-complex hydrogels for boosting redox biocatalysis, J. Mater. Chem. A. 1 (2013) 1040–1044. doi:10.1039/C2TA00358A.

[17] L. Zhang, N. Vilà, G.W. Kohring, A. Walcarius, M. Etienne, Covalent Immobilization of (2,2′-Bipyridyl) (Pentamethylcyclopentadienyl)-Rhodium Complex on a Porous Carbon Electrode for Efficient Electrocatalytic NADH Regeneration, ACS Catal. 7 (2017) 4386–4394. doi:10.1021/acscatal.7b00128.

[18] L. Zhang, N. Vilà, A. Walcarius, M. Etienne, Molecular and Biological Catalysts Coimmobilization on Electrode by Combining Diazonium Electrografting and Sequential Click Chemistry, ChemElectroChem. 5 (2018) 2208–2217. doi:10.1002/celc.201800258.

[19] L. Zhang, M. Etienne, N. Vilà, T.X.H. Le, G.-W. Kohring, A. Walcarius, Electrocatalytic Biosynthesis using a Bucky Paper Functionalized by [Cp*Rh(bpy)Cl]

+ and a Renewable Enzymatic Layer, ChemCatChem. 10 (2018) 4067–4073. doi:10.1002/cctc.201800681.

[20] A. Tosstorff, A. Dennig, A.J. Ruff, U. Schwaneberg, V. Sieber, K.M. Mangold, et al., Mediated electron transfer with monooxygenases - Insight in interactions between reduced mediators and the co-substrate oxygen, J. Mol. Catal. B Enzym. 108 (2014) 51–58. doi:10.1016/j.molcatb.2014.06.011.

[21] L. Gorton, E. Dominguez, Electrochemistry of NAD(P) + /NAD(P)H, in: Encycl. Electrochem., Wiley-VCH Verlag GmbH & Co. KGaA, Weinheim, Germany, 2007: pp. 67–143. doi:10.1002/9783527610426.bard090004.

[22] K. Andersen, T. Kjar, N.P. Revsbech, An oxygen insensitive microsensor for nitrous oxide, Sensors Actuators, B Chem. 81 (2001) 42–48. doi:10.1016/S0925-4005(01)00924-8.

[23] Y. Gu, C.C. Chen, Eliminating the interference of oxygen for sensing hydrogen peroxide with the polyaniline modified electrode, Sensors. 8 (2008) 8237–8247. doi:10.3390/s8128237.

[24] M. Swoboda, J. Henig, H.-M. Cheng, D. Brugger, D. Haltrich, N. Plumeré, et al., Enzymatic Oxygen Scavenging for Photostability without pH Drop in Single-Molecule Experiments, ACS Nano. 6 (2012) 6364–6369. doi:10.1021/nn301895c.

[25] H.B. Hanekamp, W.H. Voogt, P. Bos, R.W. Frei, An electrochemical scrubber for the elimination of eluent background effects in polarographic flow-through detection, Anal. Chim. Acta. 118 (1980) 81–86. doi:10.1016/S0003-2670(01)93716-X.

[26] E. Bertin, S. Garbarino, D. Guay, Interdigitated microelectrodes for oxygen removal in N2H4sensors, Electrochem. Commun. 71 (2016) 56–60. doi:10.1016/j.elecom.2016.08.006.

[27] M. Etienne, T.X.H. Le, T. Nasir, G. Herzog, Electrochemical Filter To Remove

Oxygen Interference Locally, Rapidly, and Temporarily for Sensing Applications, Anal. Chem. (2020) acs.analchem.0c00395. doi:10.1021/acs.analchem.0c00395.

[28] L. Hussein, G. Urban, M. Krüger, Fabrication and characterization of buckypaper-based nanostructured electrodes as a novel material for biofuel cell applications., Phys. Chem. Chem. Phys. 13 (2011) 5831–9. doi:10.1039/c0cp02254c.

[29] I. Mazurenko, M. Etienne, G.W. Kohring, F. Lapicque, A. Walcarius, Enzymatic bioreactor for simultaneous electrosynthesis and energy production, Electrochim. Acta. 199 (2016) 342–348. doi:10.1016/j.electacta.2016.02.126.

[30] M. Mierzwa, E. Lamouroux, I. Vakulko, P. Durand, M. Etienne, Electrochemistry and Spectroelectrochemistry with Electrospun Indium Tin Oxide Nanofibers, Electrochim. Acta. 202 (2016) 55–65. doi:10.1016/j.electacta.2016.03.136.

[31] A. Walcarius, R. Nasraoui, Z. Wang, F. Qu, V. Urbanova, M. Etienne, et al., Factors affecting the electrochemical regeneration of NADH by (2,2′-bipyridyl) (pentamethylcyclopentadienyl)-rhodium complexes: Impact on their immobilization onto electrode surfaces, Bioelectrochem. 82 (2011) 46–54. doi:10.1016/j.bioelechem.2011.05.002.

[32] E. Steckhan, S. Herrmann, R. Ruppert, E. Dietz, M. Frede, E. Spika, Analytical study of a series of substituted (2,2'-bipyridyl)(pentamethylcyclopentadienyl)rhodium and -iridium complexes with regard to their effectiveness as redox catalysts for the indirect electrochemical and chemical reduction of NAD(P)+, Organometallics. 10 (1991) 1568–1577. doi:10.1021/om00051a056.

[33] S.S. Yamini Satyawali, Enzymatic Electrosynthesis: An Overview on the Progress in Enzyme- Electrodes for the Production of Electricity, Fuels and Chemicals, J. Microb. Biochem. Technol. (2013). doi:10.4172/1948-5948.S6-007.

[34] F. Hildebrand, S. Lütz, Stable Electroenzymatic Processes by Catalyst Separation,

Chem. - A Eur. J. 15 (2009) 4998–5001. doi:10.1002/chem.200900219.

[35] V. Briega-Martos, E. Herrero, J.M. Feliu, Effect of pH and Water Structure on the Oxygen Reduction Reaction on platinum electrodes, Electrochim. Acta. 241 (2017) 497–509. doi:10.1016/j.electacta.2017.04.162.

[36] J.M. Noël, A. Latus, C. Lagrost, E. Volanschi, P. Hapiot, Evidence for OH radical production during electrocatalysis of oxygen reduction on pt surfaces: Consequences and application, J. Am. Chem. Soc. 134 (2012) 2835–2841. doi:10.1021/ja211663t.